Nanopore sequencing provides superior MGMT promoter methylation evaluation to conventional techniques

Skarphedinn Halldorsson *[1], Richard Nagymihaly[1], Areeba Patel [2], Petter Brandal[3], Ioannis Panagopoulos[3], Henning Leske [4], Felix Sahm [2], and Einar Vik-Mo †[1]

[1]Vilhelm Magnus Laboratory, Institute for Surgical Research, Oslo University Hospital

[2]Department of Neuropathology, University Hospital Heidelberg, Heidelberg, Germany

[3]Section for Cancer Cytogenetics, Institute for Cancer Genetics and Informatics, Oslo University Hospital

[4]Department of Pathology, Oslo University Hospital, Oslo, Norway.

Abstract

Rationale: Resistance of glioblastoma to the alkylating agent temozolomide may result from the expression of the DNA repair protein O6-methylguanine-DNA methyltransferase (*MGMT*). Methylation of the *MGMT* promoter region has been correlated with responsiveness to temozolomide, but there is no consensus on the most accurate method to determine methylation. Conventional methods have limitations such as the need for bisulphate treatment and amplification. Nanopore long-read sequencing offers methylation analysis of native DNA without the need for bisulphate treatment or amplification. Combined with recent advancements in targeting methods, it provides a modern, cost-effective approach to *MGMT* promoter methylation analysis.

Methods: In this study, we analyzed 148 CNS tumors using Nanopore sequencing and compared the results to data obtained using pyrosequencing or methylation bead arrays. We used Oxford Nanopore Technologies (ONT) MinION flow cells to run single or barcoded (multiplex) assays, following a CRISPR/Cas9 protocol, and included results from adaptive sequencing runs. We then compared the methylation data to results from standard diagnostic methods.

Results: We found a 92% correlation between pyrosequencing of 4 CpGs in the CpG island of MGMT and nanopore sequencing. We could re-create classification by the MGMT STP27 algorithm with data from nanopore sequencing. Furthermore, we were able to include

*skarphedinn.halldorsson@rr-research.no
†einar.vik-mo@rr-research.no

in the analysis an additional 94 CpGs within the MGMT CpG island and 17 CpGs within the island shores. Data clustering revealed a robust difference between unmethylated and methylated samples that could be used for patient stratification.

Discussion: Our findings demonstrate that ONT is a capable method for replacing pyrosequencing, or methylation bead-array, providing high-confidence results within a few hours of sequencing. The extension of the analysis to all of the 98 CpGs of the CpG island of the MGMT promoter region results in a complete picture of the investigated MGMT region, which potentially enables further exploration of the correlation between methylation status and additional clinical parameters . However, for full replacement of standard diagnostic methods such as pyrosequencing analysis, further studies need to be performed using nanopore sequencing to refine the treatment relevant sites and cut-off levels for methylation.

Keywords: MGMT promoter methylation, Nanopore sequencing, CRISPR/Cas9, Glioblastoma

Introduction

Glioblastoma multiforme (GBM) is the most common and most aggressive type of primary malignant brain tumor in adults [Ostrom et al., 2020] with a median survival of about 15 years [Stupp et al., 2017]. Standard treatment for GBM involves surgical resection of the tumor followed by a combination of radiation and chemotherapy. Temozolomide (TMZ) is a chemotherapy drug that has been shown to improve the outcome in a subset of GBM patients when used in combination with radiotherapy [Stupp et al., 2009]. It is an alkylating agent that induces DNA damage by methylation of O-6 guanidine residues in dividing cells, leading to DNA damage and apoptosis [Zhang et al., 2011]. Despite its potential benefits, TMZ can cause a range of side effects and should therefore be limited to patients that may benefit from it and withheld from patients that most likely will only experience the side effects without any improvement in survival [Hegi and Ichimura, 2021]. The effects of TMZ are countered by the DNA repair protein O-6 methylguanine DNA methyltransferase (MGMT). MGMT expression is regulated via methylation of the promoter region [Nakagawachi et al., 2003]. The presence of MGMT promoter methylation has been associated with increased survival in glioblastoma patients treated with temozolomide and radiation therapy [Hegi et al., 2019]. Methylation of the MGMT promoter is believed to silence its expression, thereby increasing sensitivity of GBM tumor cells to TMZ. MGMT promoter methylation status is therefore an important factor for the management and treatment of GBM [Christmann et al., 2011].

Pyrosequencing is a commonly used method to detect MGMT promoter methylation in clinical samples. The Qiagen® MGMT pyrosequencing kit, which detects methylation on 4 CpG sites (76-79) on the MGMT promoter CpG island, is a common choice in the clinical setting. However, there is neither a clear consensus on the best cut-off point to classify clinically relevant methylated or unmethylated samples, nor which method should be used [Brandner et al., 2021]. Standard diagnostic techniques include methylation-specific PCR (MSP), pyrosequencing (PSQ) or methylation bead array [Johannessen et al., 2018]. All of these methods rely on bisulfite conversion of native tumor DNA prior to analysis and only include a fraction of the 98 potentially relevant CpG sites in the CpG island of MGMT [Malley et al., 2011]. In recent years, advances in sequencing technology have allowed for more sensitive and accurate detection of DNA methylation. Nanopore sequencing, which uses a nanopore-based sensor to detect changes in electrical current as nucleic acids (DNA or RNA) pass through the pore, has the ability to detect epigenetic modifications, such as methylation, directly from the signal [Jain et al., 2016]. Due to the long-read nature of nanopore sequencing, it also affords methylation analysis of far longer sequences than either MSP or pyrosequencing. Consequently, nanopore sequencing offers an overview of the methylation status of all CpGs of the MGMT CpG-island including the promoter region, using native genomic DNA without bisulfite conversion, which can be both time and cost efficient in a clinical setting [Laver et al., 2015]. In this study, we compared the results of nanopore sequencing of the promoter region of MGMT of 148 central nervous system (CNS) tumors, including 91 GBMs, with results obtained from standard diagnostic methods comprising pyrosequencing or Illumina 850K bead array.

Materials and Methods

Patients and samples

Samples from three independent cohorts were included into this study; 1) Retrospective analysis of DNA from 68 CNS tumor samples provided by the Institute for Cancer Genetics and Informatics, Oslo University Hospital, screened for MGMT promoter methylation using the Qiagen® MGMT pyrosequencing kit. 2) Retrospective analysis of 67 sequences generated as part of the Rapid-CNS adaptive sampling pipeline [Patel et al., 2022] analysed by Illumina® methylation 850K bead array. 3) DNA extracted from 16 glioma biopsies that were operated at Oslo Uni-

versity Hospital. A separate biopsy derived from paraffin-embedded tissue was analysed with the Qiagen® MGMT pyrosequencing kit at the Dept of Molecular Pathology Table 1 provides an overview of samples used in this study.

A total of 153 samples from 148 patients were analyzed for MGMT promoter methylation, consisting of 91 GBM samples, 23 IDH-glioma samples, and 12 meningioma samples (Figure 2a). Two methods were used to enrich for the region of interest: CRISPR/Cas9 targeted sequencing of the MGMT promoter region [Wongsurawat et al., 2020] and adaptive sampling. Cas9 targeted sequencing was applied to 86 samples, 46 of which were run as single samples and 40 that were run as multiplexed groups of five. 67 samples were analyzed as part of an adaptive sampling pipeline.

Sample preparation and Nanopore sequencing

Between 10 and 25 mg of fresh/frozen tissue were used to extract genomic DNA (Merck's GenElute™ Mammalian Genomic DNA Miniprep kit) following the manufacturer's protocol. Purity and concentration of DNA samples was determined using NanoDrop™ One and Qubit™ 4 Fluorometers (Thermo Fischer Scientific). Isolated DNA was stored at -20°C until analysis. Cas9 mediated targeted sequencing was performed with the Cas9 Sequencing Kit (Oxford Nanopore Technologies) according to the manufacturers protocol (version ENR 9084 v109 revR 04Dec2018). Briefly, Cas9 ribonucleoprotein complexes (RNPs) were created by mixing equimolar concentrations (100 µM) of crispr RNA (crRNA) and trans-activating elements (tracrRNA) to HiFi Cas9 enzyme (IDT). Dephosphorylated gDNA (2-5 µg) was cleaved and dA-tailed with Cas9 RNPs and Taq polymerase. Finally, sequencing adaptors were ligated to the cleaved fragments and the final DNA library was purified with AMPure XP beads (Beckman Coulter). Barcodes were applied to a number of samples to allow multiplexing of five samples based on an experimental protocol from Oxford Nanopore Technologies. Purified DNA libraries were loaded onto R9.4.1. flow cells on MinION Mk1B or Mk1C devices and sequenced for 4-24 hours. Individual flow cells were flushed and re-used up to four times for single samples and twice for multiplexed samples. A minimum pore-count of 300 was deemed sufficient for a single sample, 800 for multiplexed samples. Raw fast5 sequences of all fragments mapping to the MGMT promoter in the Rapid-CNS data were provided for re-analysis.

Primers

All primers were purchased from Integrated DNA Technologies, IDT (Leuven, Belgium). Previously published primers were initially used to target the MGMT promoter [Wongsurawat et al., 2020], termed MGMT-left-1 (ATGAGGGGCCCACTAATTGA) and MGMT-right-1 (ACCTGAGTATAGCTCCGTAC), which yielded produced a fragment of 2,522 bp. In order to increase cas9 efficiency and expand the size of the fragment, we added additional crRNA primers: MGMT-left-2 (GCCAACCACGTTAGAGACAATGG), MGMT-right-2 (GTACGGAGCTATACTCAGGT), MGMT-right3 (CTGGAATCGCATTCCAGTAGTGG) and MGMT-right-4 (ACTTCGCAAGCATCACAGGTAGG) providing a fragment of 4,800 bp.

Data analysis

Raw sequences were base-called, methylation called and mapped (hg19, chromosome 10) using the Megalodon toolbox (version 2.5.0 built on guppy version 6.2.7) from Oxford Nanopore Technologies (https://github.com/nanoporetech/megalodon). Methylation percentages of individual CpG sites were compiled using custom scripts in R. All statistical analyses were performed in R (version 4.2.1). The source code and data to reproduce all analyses and figures from this manuscript is available at https://github.com/SkabbiVML/MGMT_R.

Results

Data acquisition

Sequence depth of the MGMT promoter region in the samples varied based on method, sequencing time, and DNA and flow-cell quality. Single sample runs produced on average more sequences (mean = 92.1, median = 33) than barcoded runs (mean = 17.2, median = 12) and adaptive sampling (mean = 18.7, median = 15) (Figure 2b). No bias in sequencing depth was observed between methylated and unmethylated samples across Cas9 targeted samples, either single or multiplexed. However, a slight but statistically significant difference in sequence depth was observed between methylated (mean = 23.6) and unmethylated (mean = 16.5) samples created by adaptive sampling (p=0.021).

Nanopore Sequencing versus Pyrosequencing of the MGMT Promoter

A subset of our samples (n=68) were initially analyzed using the Qiagen® MGMT pyrosequencing kit (MGMT pyro kit)), which investigates the CpGs 76-79 of the CpG island of MGMT, before undergoing nanopore sequencing. . This allowed a direct comparison of the results of the MGMT pyro kit with those of the nanopore sequencing covering the same CpG sites (Figure 3). The correlation between the methylation values of each overlapping CpG site between nanopore and pyrosequencing ranged from 0.78 to 0.88 (Figure 3a). However, the correlation increased to 0.92 when methylation values were averaged across the four CpG sites (Figure 3b).

At Oslo University Hospital an average methylation of 10% and above using the Qiagen® MGMT pyrosequencing kit is considered to be methylated. 10%average methylation threshold of CpGs 76-79 was applied to the nanopore data to re-classify MGMT methylated versus unmethylated samples. When comparing the results obtained from nanopore sequencing and pyrosequencing (Figure 3c, left), we found a 91% concordance rate between the two methods (62 out of 68 samples) (Figure 3d, upper). Notably, discordant results between nanopore sequencing and the MGMT pyro kit were in all cases classified as methylated by nanopore sequencing but unmethylated by pyrosequencing.

. When the same 10% methylation threshold of CpGs 76-79 was applied toused to re-classify samples from the adaptive sequencing panel that were previously classified by Illumina® methylation 850K bead array (n=67), the concordance between classification methods dropped to 86% (Figure 3c, right). Discordant cases between nanopore sequencing and bead array were both false positives and false negatives(Figure 3d, lower).

Illumina® Human Methylation BeadChips (HM-27K, HM-450K, and HM-850K) are microarray-based platforms used to investigate DNA methylation patterns in human tumor samples. Despite detecting the methylation status of tens to hundreds of thousands of CpG sites, these platforms only cover a fraction of the approximately 30 million CpG sites in the human genome. To predict the clinically relevant methylation status of the MGMT promoter, a regression model called *MGMT STP-27* has been developed. This model uses the methylation status of two CpG sites, cg12434587 and cg12981137, as reported by [Bady et al., 2012, Bady et al., 2016].

In the Rapid-CNS study, samples were analyzed by methylation bead array before nanopore sequencing, and the ground truth for MGMT promoter methylation status was inferred from

EPIC array results. Methylation values for the two CpG sites represented in the MGMT-STP27 algorithm were extracted from the nanopore data and plotted against each other (Figure 4a). The samples from the Rapid-CNS cohort showed a clear separation between methylated and unmethylated samples based on the methylation percentages of cg12434587 and cg12981137 (Figure 4a, right). In contrast, the samples from the Radium cohort, which were classified as methylated or unmethylated by pyrosequencing, did not show as clear a distinction regarding methylation of the STP27 sites (Figure 4a, left).

We therefore also followed the approach by Siller et. al, who proposed a method for GBM patient stratification by counting the methylation of the 25 CpG sites of the second differentially methylated region (DMR2) in the CpG island of MGMT using Sanger bisulfite sequencing [Siller et al., 2021]. The results of nanopore sequencing were binarized by applying a methylation cut-off of 10% to each CpG site (≥ 10% methylation = methylated, < 10% methylation = unmethylated) and summarizing the counts in DMR2. Figure 4b shows a nearly complete separation of methylated and unmethylated samples at $\geq$ 15 methylated CpG sites in all samples.

Unsupervised clustering of samples based on nanopore sequencing

Although classification by bisulphite sequencing methods can be recreated to a reasonable degree with nanopore sequencing data, this does not take advantage of other CpG sites within the designated MGMT promoter CpG island or its shelves and shores that may prove to be relevant for MGMT gene expression. To investigate the impact of methylation at CpG sites not covered by previous methods, we performed hierarchical clustering of 98 CpG sites on the CpG island and included 7 CpGs upstream and 11 CpGs downstream of the CpG island. Unsupervised hierarchical clustering using Ward's method reveals two main clusters that largely correspond to the classification into methylated and unmethylated samples by pyrosequencing or methylation bead array (Figure 5a).

Unmethylated samples exhibit low methylation levels throughout the CpG island, except for the first 5 CpG sites, which are often methylated. On the other hand, methylated samples show a larger gradient of methylation, with higher levels towards either end of the CpG island. This is further supported by the average methylation percentage of each CpG site in methylated and unmethylated samples (Figure 5b), which reveals the biggest differences in methylation occur

in CpGs 6 through 15 and 71 through 90.

While five samples previously classified as methylated cluster with the otherwise unmethylated samples, one unmethylated sample clusters with methylated samples. This pattern of separation is also evident when unsupervised clustering is performed on GBM samples only (Figure 6a).

In addition to the robust separation of samples into clusters that largely correspond to the predetermined methylation status, k-means clustering showed separation of samples in the methylated cluster (Figure 6b). Of the 22 samples that cluster with methylated samples, 9 samples fall within what can be described as "very high methylation" cluster. The functional significance of these clusters remains to be determined.

Survival Analysis

The methylation status of the MGMT promoter is a well-known predictive factor for the overall and progression-free survival of GBM patients receiving Temazolamide treatment [Dovek et al., 2019]. While nanopore methylation profiles were often in agreement with bisulphite sequencing methods, discrepancies were also observed (Figure 5a). Therefore, we investigated whether clustering by nanopore sequencing was as effective as the MGMT-pyro kit or EPIC-array for survival prediction. We conducted cas9-targeted nanopore sequencing on 16 additional samples that were simultaneously analyzed by pyrosequencing. In total, we performed survival analysis on 25 primary IDH negative GBM patients (11 females, average age 58.4 years and 14 males, average age 62.7 years) where biopsies were classified by both MGMT-pyro kit and cas9-targeted nanopore sequencing (Table 3).

As expected, Kaplan-Meier survival analysis of patients based on pyrosequencing showed a significantly longer overall survival in patients classified as "Methylated" (Figure 7a, p=0.0078). Notably, when patients were classified according to unsupervised clustering by nanopore sequencing (Figure 7b), significantly longer survival was observed in "cluster 2" patients (p=0.039). Although the sample size is small, our results suggest that classifying patients via nanopore sequencing is equally reliable as classification with the MGMT-pyro kit.

Discussion

This study analyzed 145 CNS tumors using targeted nanopore sequencing and compared the results to pyrosequencing and methylation bead arrays. The study found a 92% correlation be-

tween pyrosequencing and nanopore sequencing, but noted that samples with low methylation were sometimes overestimated with nanopore sequencing. Results of the MGMT STP27 algorithm could be recreated with nanopore sequencing, and the method allowed for the analysis of an additional 94 CpGs in the MGMT promoter region. Unsupervised hierarchical clustering of samples based on nanopore methylation data including 115 CpGs in and adjacent to the MGMT promoter showed clear separation of methylated and unmethylated samples. Finally, we showed that classification of patients by targeted nanopore sequencing of the MGMT promoter yielded results that were comparable to pyrosequencing. To the best of our knowledge, this is the first study to examine all 98 sites with the MGMT promoter CpG island, along with it's shores in multiple patient biopsies.

MGMT promoter methylation by nanopore sequencing has two main advantages over conventional techniques. First, nanopore sequencing can detect epigenetic modifications on native DNA, thereby circumventing the need for bisulfite treatment. This saves time and reduces the potential risk of bias introduced by bisulfite treatment that has been shown to under represent densely hydroxymethylated (5hmC) regions [Huang et al., 2010]. Secondly, the long-read nature of nanopore sequencing offers a complete overview of the MGMT promoter CpG island and can be extended in either direction to include the shores and shelves of the CpG island. We conclude that nanopore sequencing of the MGMT promoter region performs as well or better than standard methods such as pyrosequencing. This is true for both cas9 targeted sequencing of the MGMT promoter and inclusion of the MGMT promoter into an adaptive sequencing panel. Distinct subgroups within both methylated and unmethylated samples were observed via nanopore sequencing although any difference in patient outcome between these clusters has yet to be determined.

Tables

Table 1: Summary of samples included in this study.

	DenStem	Radium	Rapid-CNS	Total
Astrocytoma	3	1	3	7
Astrocytoma HG	0	4	4	8
Pilocytic astrocytoma	0	0	4	4
Glioblastoma	13	29	49	91
Meningioma	0	12	0	12
Metastasis	0	7	0	7
Oligodendroglioma	0	2	6	8
Other	0	10	1	11
Total	16	65	67	148

Table 2: Summary of reported optimal cut-offs for determining methylated versus unmethylated samples

Author	Year	Method	Patients	CpGs	Optimal cut-off	Comment	Reference
Hegi	2019	qMSP	4041		>1.27	”Grey-zone” patients benefit from TMZ	[Hegi et al., 2019]
Johannessen	2018	qMSP, PSQ	48		7 %	PSQ gives better results than other methods	[Johannessen et al., 2018]
Nguyen	2021	PSQ	109		21 %	Higher methylation corrilates with longer OS	[Nguyen et al., 2021]
Quillien	2012	MSP, PSQ, MS-HRM	100	5	8 %	PSQ performs best	[Quillien et al., 2012]
Xie	2015	PSQ	43		10 %	Not testing cut-off	[Xie et al., 2015]
Yuan	2017	PSQ	84	4	12.50 %	Higher methylation corrilates with longer OS	[Yuan et al., 2017]
Brigliadori	2016	PSQ	105	10	30 %	”Grey-zone” patients do not benefit from TMZ	[Brigliadori et al., 2016]
Radke	2019	PSQ, sqMSP	111		10 %	Best results when PSQ and MSP were combined	[Radke et al., 2019]
Chai	2021	PSQ	173	4	10 %	MGMT promoter methylation has predictive value in IDH-mutant glioblastoma	[Choi et al., 2021]
Dovek	2019	qMSP	165		>1	”Grey-zone” patients benefit from TMZ, higher methylation does not correlate with longer OS	[Dovek et al., 2019]
Siller	2021	MSP, Sseq	215	25		Linear correlation between number of methylated CpG sites and OS	[Siller et al., 2021]

Table 3: Patients used in survival analysis

Sample ID	Age	Sex	Diagnosis	IDH	Resection	Treatment	OS (months)	Status	Pyro_state	NP cluster
1701-2275	66	F	GBM	Neg	GTR	Stupp	14.99	Dead	UnMethylated	1
1701-2430	78	M	GBM	Neg	GTR	Stupp	5.19	Dead	Methylated	2
1701-2590	58	M	GBM	Neg	STR	Stupp	24.5	Dead	Methylated	2
1701-2623	57	F	GBM	Neg	STR	Stupp	28.77	Dead	Methylated	2
1701-2769	73	M	GBM	Neg	STR	Stupp	20.91	Dead	UnMethylated	1
1701-2950	77	M	GBM	Neg	STR	Stupp	11.97	Dead	UnMethylated	1
1501-1486	60	M	GBM	Neg	GTR	Stupp	29.26	Dead	Methylated	2
1501-1757	65	M	GBM	Neg	STR	Stupp	29.69	Dead	Methylated	2
1501-1858	62	F	GBM	Neg	STR	Stupp	6.9	Dead	UnMethylated	1
1501-1880	64	M	GBM	Neg	STR	Stupp	25.48	Dead	Methylated	2
1501-2159	58	M	GBM	Neg	STR	Stupp	21.6	Dead	Methylated	2
1501-2348	58	M	GBM	Neg	STR	Stupp	11.44	Dead	UnMethylated	1
1501-2391	72	F	GBM	Neg	STR	Stupp	21.21	Dead	Methylated	2
1501-2425	58	F	GBM	Neg	STR	Stupp	13.61	Dead	Methylated	2
1601-0227	66	M	GBM	Neg	STR	Stupp	21.96	Dead	Methylated	2
1601-0353	51	M	GBM	Neg	GTR	Stupp	12.85	Dead	Methylated	2
T20-061	64	F	GBM	Neg	STR	Stupp	8.3	Dead	Methylated	1
T20-192	52	F	GBM	Neg	STR	Stupp	23	Dead	Methylated	2
T21-173	66	F	GBM	Neg	STR	Stupp	13.6	Dead	Methylated	2
T21-214	49	M	GBM	Neg	GTR	Stupp	9.4	Dead	UnMethylated	1
T21-216	46	F	GBM	Neg	GTR	Stupp	14.31	Alive	Methylated	2
T21-224	60	F	GBM	Neg	GTR	Stupp	14.08	Alive	Methylated	1
T21-240	55	M	GBM	Neg	GTR	Stupp	15.16	Alive	UnMethylated	2
T21-242	66	M	GBM	Neg	GTR	Stupp	14.47	Alive	Methylated	2
T21-326	39	F	GBM	Neg	GTR	Stupp	13.78	Alive	Methylated	1

Figures

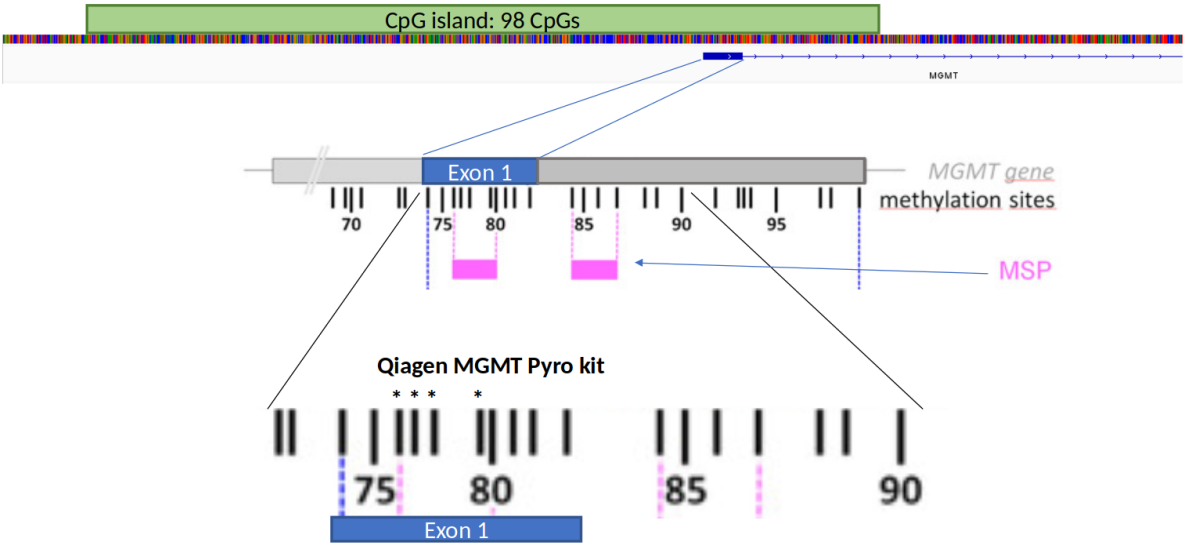

Figure 1: Organization of the MGMT promoter. MSP refers to the typical primer sites of methylation specific PCR to determine MGMT promoter methylation. Asterixes represent the 4 CpGs analysed by the Qiagen® MGMT pyrosequencing kit.

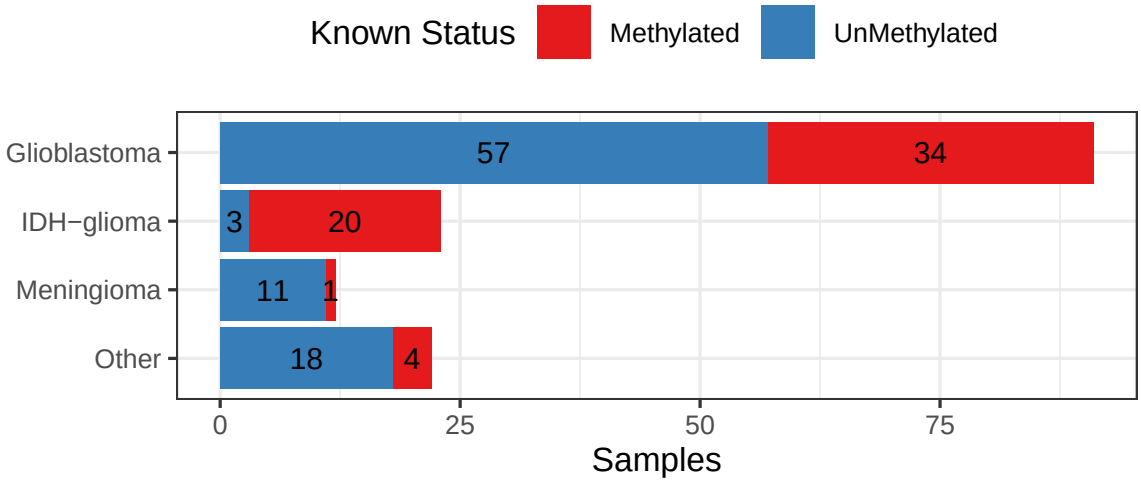

(a)

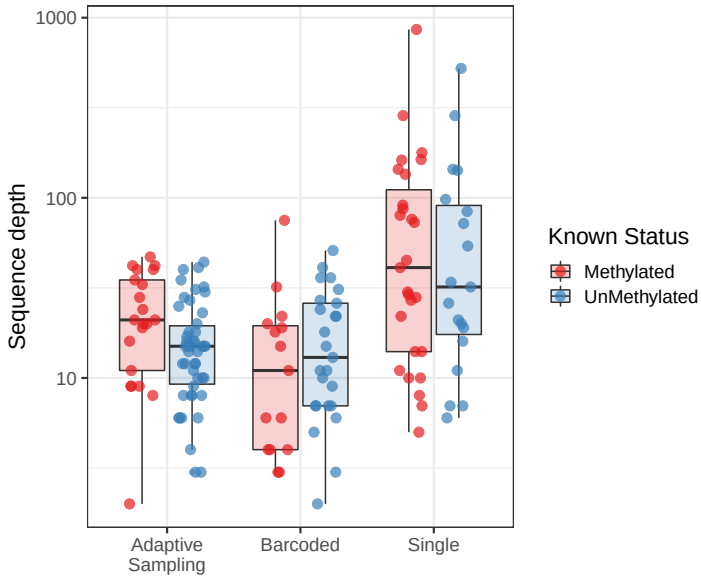

(b)

Figure 2: Overview of samples and sequence depth. (a) Classification of all samples used in this study, separated by known methylation status (b) Methylated versus unmethylated samples by method of acquisition (Adaptive sampling, multiplexed nCats, single sample nCats). No bias in sequence depth was observed between methylated and unmethylated samples but single sample runs generally have higher sequence depth than barcoded samples or adaptive sampling.

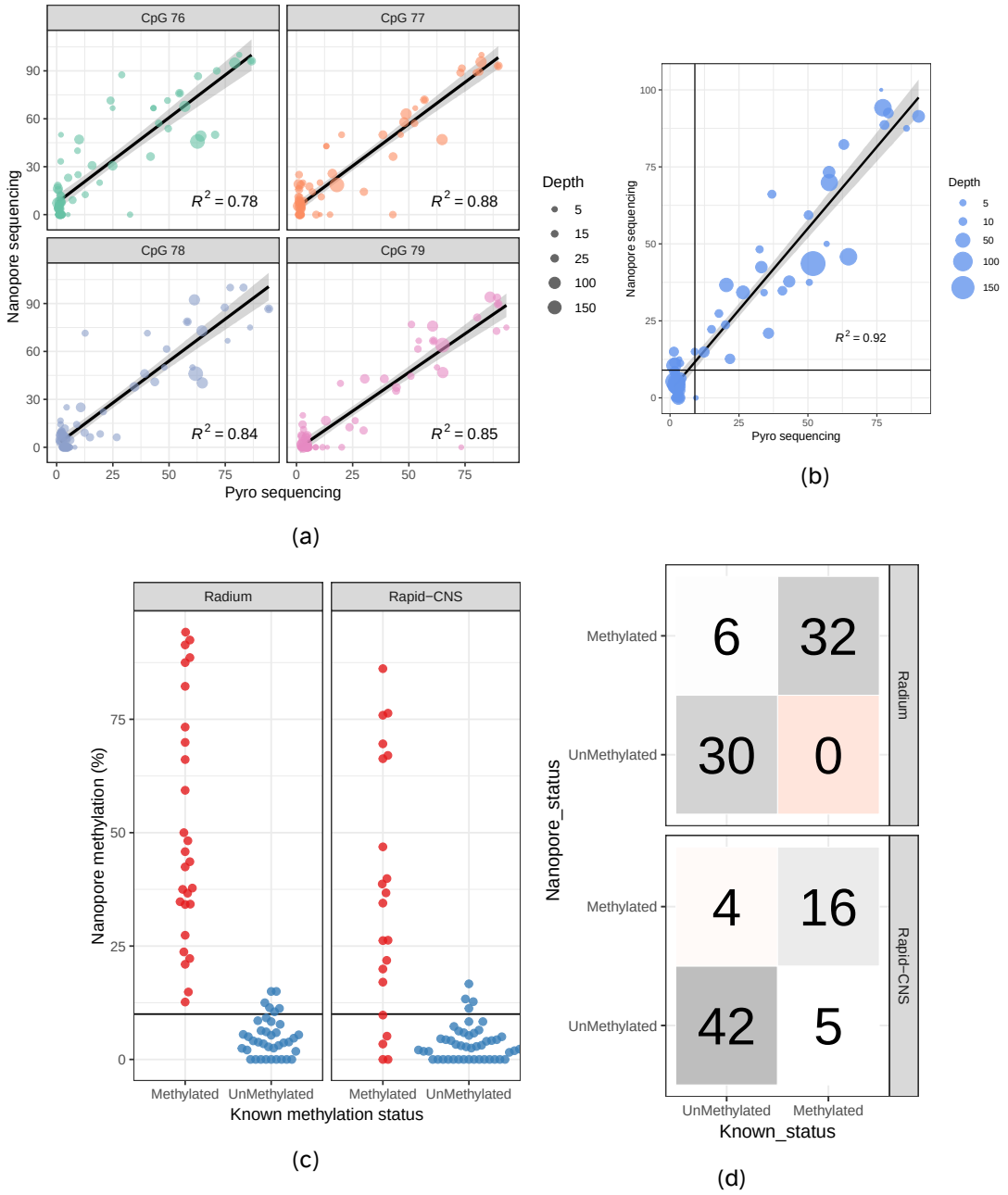

Figure 3: Comparison of nanopore sequencing and Qiagen® Pyrosequencing kit of CpGs 76-79 in exon 1 of the MGMT promoter. Results show per-site methylation percentage of each CpG (a) or average values of the 4 CpG sites analysed by the Qiagen® MGMT Pyro kit. Black horizontal and vertical lines mark the 10 % cut-off value between methylated and unmethylated samples, as determined by pyrosequencing. Comparison of pyrosequencing classification into methylated versus unmethylated based on a 10% average methylation threshold of CpGs 76-79 in the MGMT promoter (c). The Y-axis represents average methylation percentage of the same four CpG sites based on nanopore sequencing.

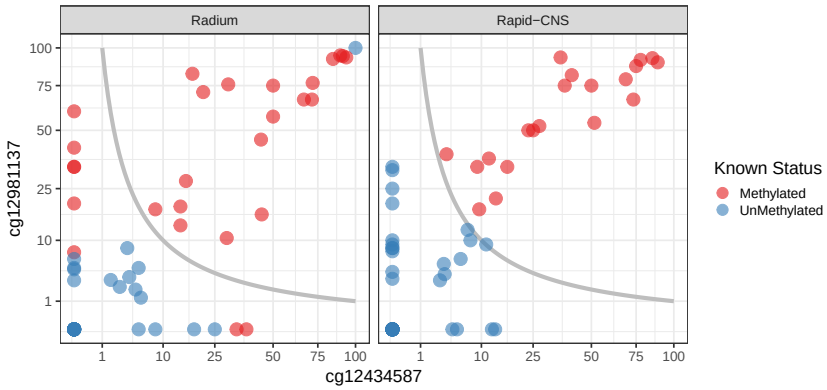

(a)

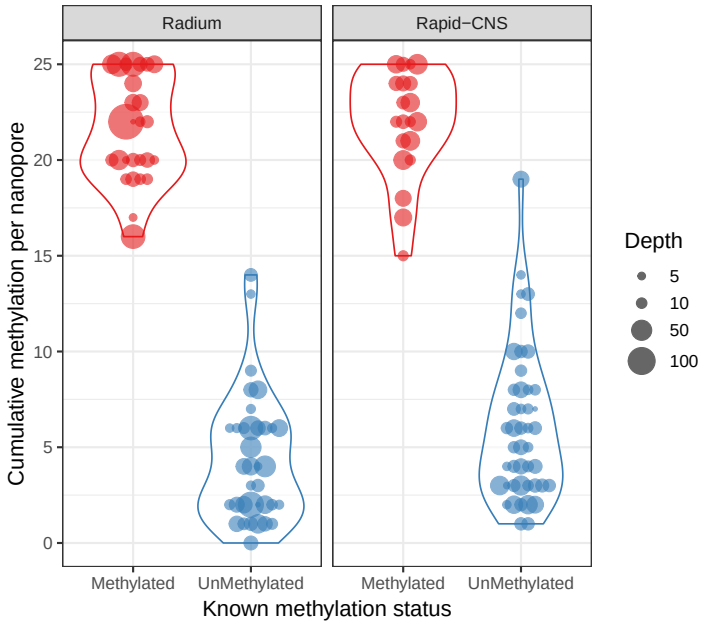

(b)

Figure 4: Something about classifying tumor by an algorithm that only uses 2 CpGs (a). Something about how the different datasets classify differently (b). Something about classifying and sub-classifying tumors according to the methylation of the last 25 CpGs in the MGMT promoter region, as was proposed by Siller *et al.* [Siller et al., 2021] (c). The Y-axis represents aggregated methylation og CpGs 74 to 98 by Nanopore sequencing.

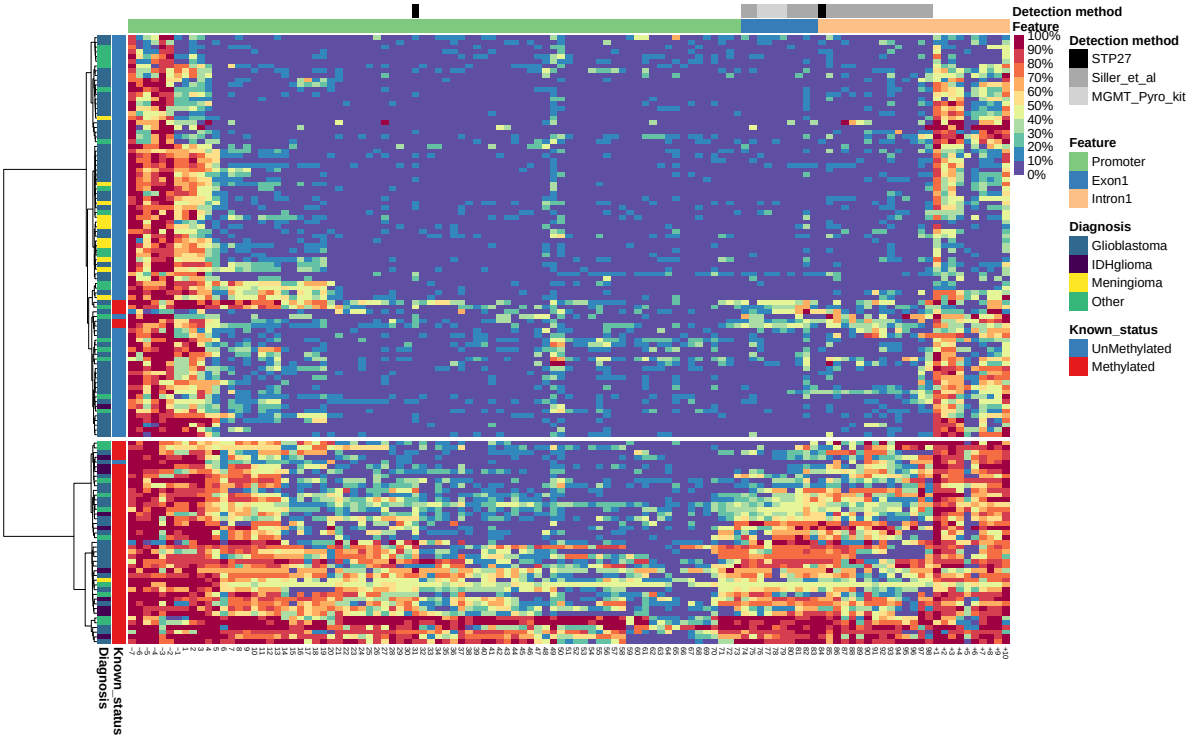

(a)

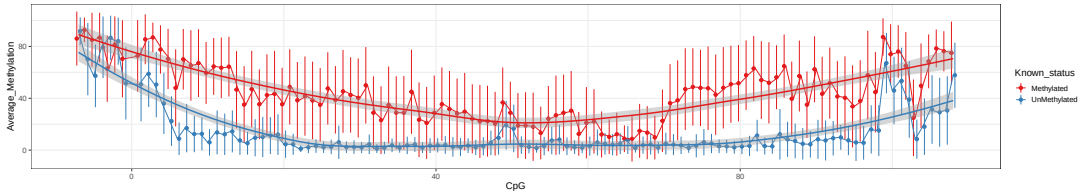

(b)

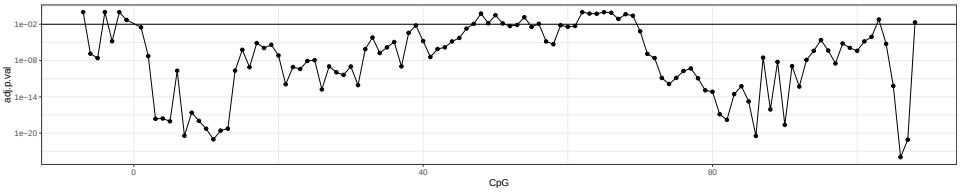

(c)

Figure 5: a) Clustered heatmap of all samples based on nanopore sequencing of CpG island of the MGMT promoter. n = 128. b) Dotplot showing average methylation percentage of CpG sites in and around the MGMT promoter. Error bars represent standard deviation, grey areas show 95% confidence intervals of regression lines, n = 128. c) Dotplot showing Bonferroni adjusted p-values of Welch's two-sided t-test for every CpG site. Horizontal line depicts 0.01.

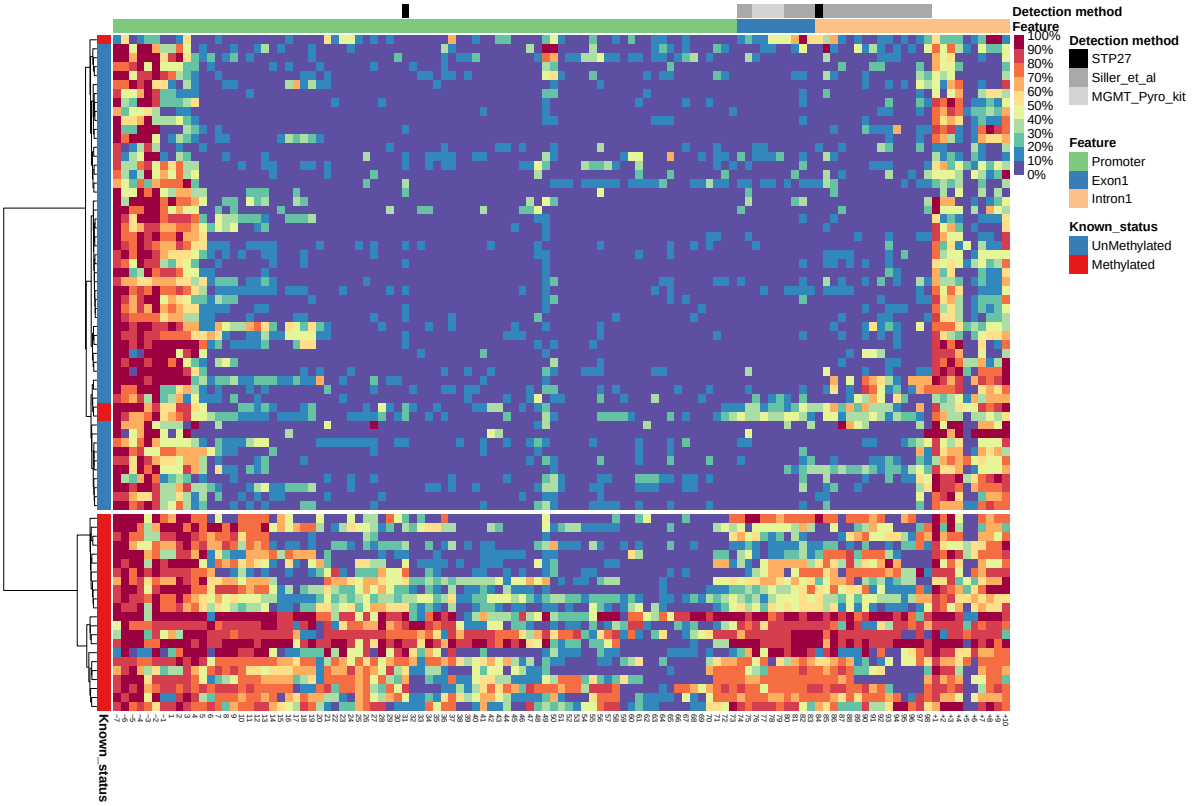

(a)

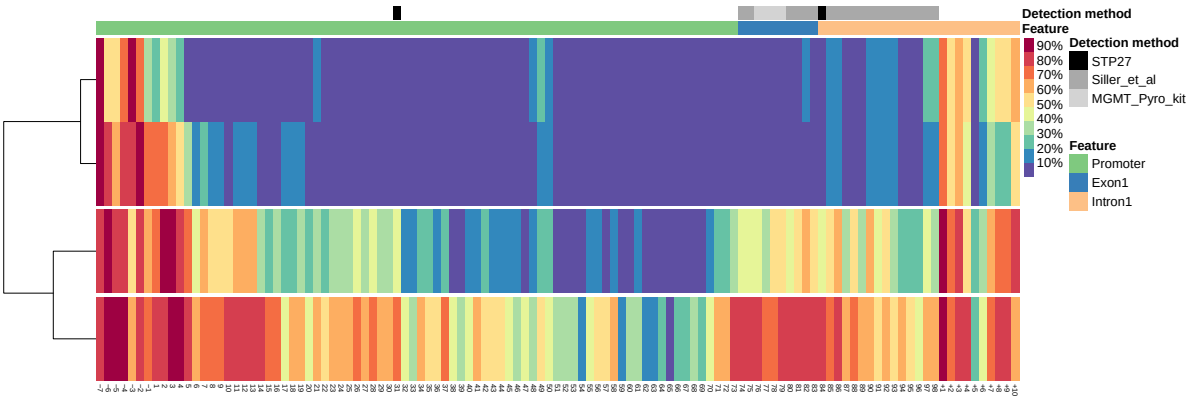

(b)

Figure 6: a) Heatmap showing unsupervised clustering of glioblastoma samples based on nanopore sequencing of the CpG island in the MGMT promoter. n = 78. b) K-means clustering of glioblastoma samples.

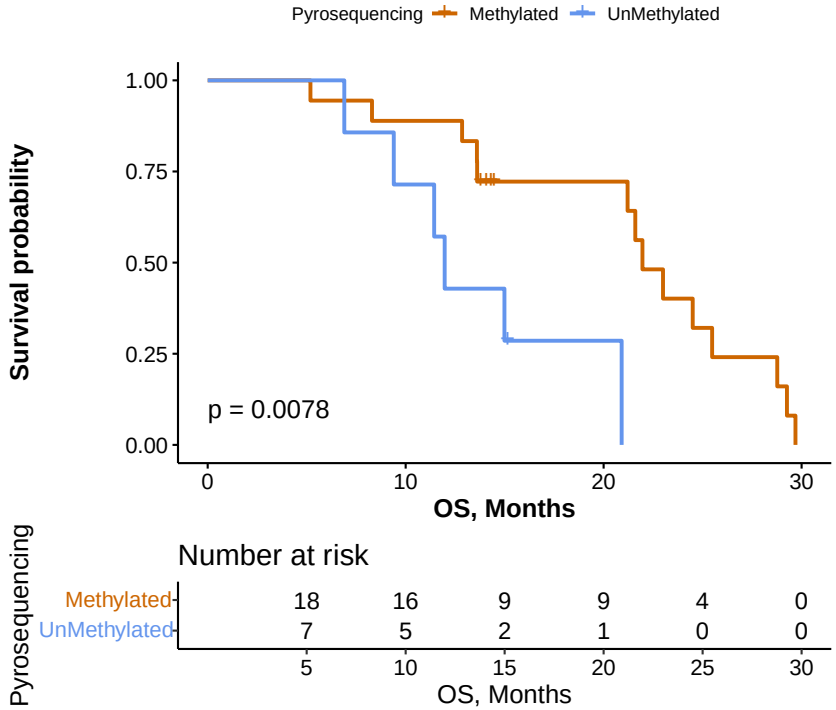

(a) Pyro classification

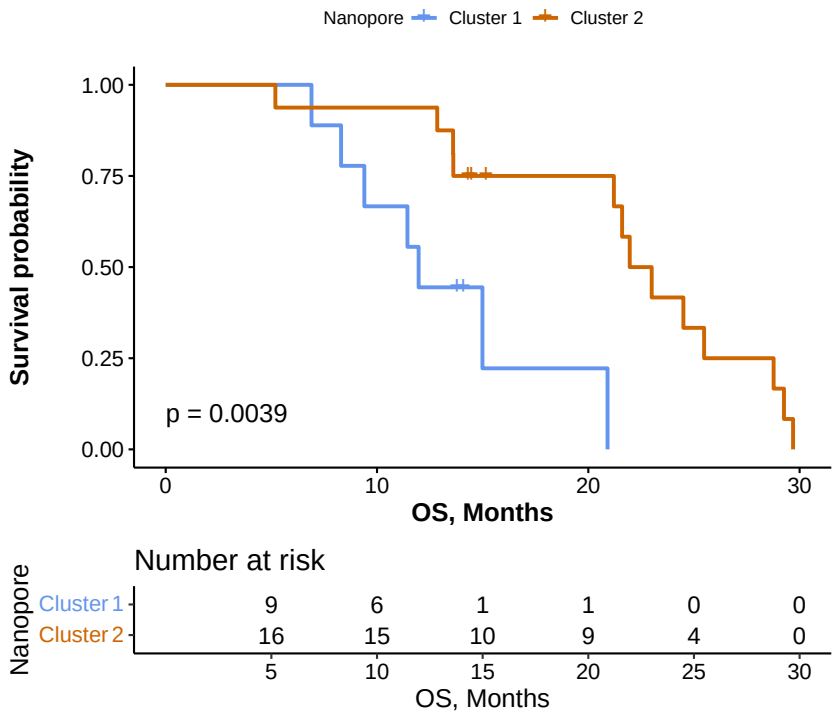

(b) Nano Classification

Figure 7: Patient survival based on Pyrosequencing classification (a) or Nanopore Sequencing classification (b)

References

[Bady et al., 2016] Bady, P., Delorenzi, M., and Hegi, M. E. (2016). Sensitivity Analysis of the MGMT-STP27 Model and Impact of Genetic and Epigenetic Context to Predict the MGMT Methylation Status in Gliomas and Other Tumors. *Journal of Molecular Diagnostics*, 18(3).

[Bady et al., 2012] Bady, P., Sciuscio, D., Diserens, A. C., Bloch, J., Van Den Bent, M. J., Marosi, C., Dietrich, P. Y., Weller, M., Mariani, L., Heppner, F. L., Mcdonald, D. R., Lacombe, D., Stupp, R., Delorenzi, M., and Hegi, M. E. (2012). MGMT methylation analysis of glioblastoma on the Infinium methylation BeadChip identifies two distinct CpG regions associated with gene silencing and outcome, yielding a prediction model for comparisons across datasets, tumor grades, and CIMP-status. *Acta neuropathologica*, 124(4):547–560.

[Brandner et al., 2021] Brandner, S., McAleenan, A., Kelly, C., Spiga, F., Cheng, H. Y., Dawson, S., Schmidt, L., Faulkner, C. L., Wragg, C., Jefferies, S., Higgins, J. P., and Kurian, K. M. (2021). MGMT promoter methylation testing to predict overall survival in people with glioblastoma treated with temozolomide: A comprehensive meta-analysis based on a Cochrane Systematic Review. *Neuro-Oncology*, 23(9):1457–1469.

[Brigliadori et al., 2016] Brigliadori, G., Foca, F., Dall'Agata, M., Rengucci, C., Melegari, E., Cerasoli, S., Amadori, D., Calistri, D., and Faedi, M. (2016). Defining the cutoff value of MGMT gene promoter methylation and its predictive capacity in glioblastoma. *Journal of Neuro-Oncology*, 128(2).

[Choi et al., 2021] Choi, H. J., Choi, S. H., You, S. H., Yoo, R. E., Kang, K. M., Yun, T. J., Kim, J. H., Sohn, C. H., Park, C. K., and Park, S. H. (2021). MGMT promoter methylation status in initial and recurrent glioblastoma: Correlation study with DWI and DSC PWI features. *American Journal of Neuroradiology*, 42(5).

[Christmann et al., 2011] Christmann, M., Verbeek, B., Roos, W. P., and Kaina, B. (2011). O6-Methylguanine-DNA methyltransferase (MGMT) in normal tissues and tumors: Enzyme activity, promoter methylation and immunohistochemistry. *Biochimica et Biophysica Acta (BBA) - Reviews on Cancer*, 1816(2):179–190.

[Dovek et al., 2019] Dovek, L., Nguyen, N. T., Ozer, B. H., Li, N., Elashoff, R. M., Green, R. M., Liau, L., Leia Nghiemphu, P., Cloughesy, T. F., and Lai, A. (2019). Correlation of commercially avail-

able quantitative MGMT (O-6-methylguanine-DNA methyltransferase) promoter methylation scores and GBM patient survival. *Neuro-Oncology Practice*, 6(3).

[Hegi et al., 2019] Hegi, M. E., Genbrugge, E., Gorlia, T., Stupp, R., Gilbert, M. R., Chinot, O. L., Burt Nabors, L., Jones, G., Van Criekinge, W., Straub, J., and Weller, M. (2019). MGMT promoter methylation cutoff with safety margin for selecting glioblastoma patients into trials omitting temozolomide: A pooled analysis of four clinical trials. *Clinical Cancer Research*, 25(6):1809–1816.

[Hegi and Ichimura, 2021] Hegi, M. E. and Ichimura, K. (2021). MGMT testing always worth an emotion. *Neuro-Oncology*, 23(9):1417.

[Huang et al., 2010] Huang, Y., Pastor, W. A., Shen, Y., Tahiliani, M., Liu, D. R., and Rao, A. (2010). The behaviour of 5-hydroxymethylcytosine in bisulfite sequencing. *PLoS ONE*, 5(1).

[Jain et al., 2016] Jain, M., Olsen, H. E., Paten, B., and Akeson, M. (2016). The Oxford Nanopore MinION: Delivery of nanopore sequencing to the genomics community. *Genome Biology*, 17(1).

[Johannessen et al., 2018] Johannessen, L. E., Brandal, P., Myklebust, T. ., Heim, S., Micci, F., and Panagopoulos, I. (2018). MGMT gene promoter methylation status – Assessment of two pyrosequencing kits and three methylation-specific PCR methods for their predictive capacity in glioblastomas. *Cancer Genomics and Proteomics*, 15(6):437–446.

[Laver et al., 2015] Laver, T., Harrison, J., O'Neill, P. A., Moore, K., Farbos, A., Paszkiewicz, K., and Studholme, D. J. (2015). Assessing the performance of the Oxford Nanopore Technologies MinION. *Biomolecular Detection and Quantification*, 3.

[Malley et al., 2011] Malley, D. S., Hamoudi, R. A., Kocialkowski, S., Pearson, D. M., Collins, V. P., and Ichimura, K. (2011). A distinct region of the MGMT CpG island critical for transcriptional regulation is preferentially methylated in glioblastoma cells and xenografts. *Acta Neuropathologica*, 121(5).

[Nakagawachi et al., 2003] Nakagawachi, T., Soejima, H., Urano, T., Zhao, W., Higashimoto, K., Satoh, Y., Matsukura, S., Kudo, S., Kitajima, Y., Harada, H., Furukawa, K., Matsuzaki, H., Emi, M., Nakabeppu, Y., Miyazaki, K., Sekiguchi, M., and Mukai, T. (2003). Silencing effect of CpG island

hypermethylation and histone modifications on O6-methylguanine-DNA methyltransferase (MGMT) gene expression in human cancer. *Oncogene*, 22(55).

[Nguyen et al., 2021] Nguyen, N., Redfield, J., Ballo, M., Michael, M., Sorenson, J., Dibaba, D., Wan, J., Ramos, G. D., and Pandey, M. (2021). Identifying the optimal cutoff point for MGMT promoter methylation status in glioblastoma. *CNS Oncology*, 10(3).

[Ostrom et al., 2020] Ostrom, Q. T., Patil, N., Cioffi, G., Waite, K., Kruchko, C., and Barnholtz-Sloan, J. S. (2020). CBTRUS statistical report: Primary brain and other central nervous system tumors diagnosed in the United States in 2013-2017. *Neuro-Oncology*, 22(Supplement_1):IV1–IV96.

[Patel et al., 2022] Patel, A., Dogan, H., Payne, A., Krause, E., Sievers, P., Schoebe, N., Schrimpf, D., Blume, C., Stichel, D., Holmes, N., Euskirchen, P., Hench, J., Frank, S., Rosenstiel-Goidts, V., Ratliff, M., Etminan, N., Unterberg, A., Dieterich, C., Herold-Mende, C., Pfister, S. M., Wick, W., Loose, M., von Deimling, A., Sill, M., Jones, D. T., Schlesner, M., and Sahm, F. (2022). Rapid-CNS2: rapid comprehensive adaptive nanopore-sequencing of CNS tumors, a proof-of-concept study. *Acta neuropathologica*, 143(5):609–612.

[Quillien et al., 2012] Quillien, V., Lavenu, A., Karayan-Tapon, L., Carpentier, C., Labussiäre, M., Lesimple, T., Chinot, O., Wager, M., Honnorat, J., Saikali, S., Fina, F., Sanson, M., and Figarella-Branger, D. (2012). Comparative assessment of 5 methods (methylation-specific polymerase chain reaction, methylight, pyrosequencing, methylation-sensitive high-resolution melting, and immunohistochemistry) to analyze O6-methylguanine-DNA- methyltranferase in a series of 100 glioblastoma patients. *Cancer*, 118(17).

[Radke et al., 2019] Radke, J., Koch, A., Pritsch, F., Schumann, E., Misch, M., Hempt, C., Lenz, K., Löbel, F., Paschereit, F., Heppner, F. L., Vajkoczy, P., Koll, R., and Onken, J. (2019). Predictive MGMT status in a homogeneous cohort of IDH wildtype glioblastoma patients. *Acta neuropathologica communications*, 7(1).

[Siller et al., 2021] Siller, S., Lauseker, M., Karschnia, P., Niyazi, M., Eigenbrod, S., Giese, A., and Tonn, J. C. (2021). The number of methylated CpG sites within the MGMT promoter region linearly correlates with outcome in glioblastoma receiving alkylating agents. *Acta neuropathologica communications*, 9(1):35.

[Stupp et al., 2009] Stupp, R., Hegi, M. E., Mason, W. P., van den Bent, M. J., Taphoorn, M. J., Janzer, R. C., Ludwin, S. K., Allgeier, A., Fisher, B., Belanger, K., Hau, P., Brandes, A. A., Gijtenbeek, J., Marosi, C., Vecht, C. J., Mokhtari, K., Wesseling, P., Villa, S., Eisenhauer, E., Gorlia, T., Weller, M., Lacombe, D., Cairncross, J. G., and Mirimanoff, R. O. (2009). Effects of radiotherapy with concomitant and adjuvant temozolomide versus radiotherapy alone on survival in glioblastoma in a randomised phase III study: 5-year analysis of the EORTC-NCIC trial. *The Lancet Oncology*, 10(5).

[Stupp et al., 2017] Stupp, R., Taillibert, S., Kanner, A., Read, W., Steinberg, D. M., Lhermitte, B., Toms, S., Idbaih, A., Ahluwalia, M. S., Fink, K., Di Meco, F., Lieberman, F., Zhu, J. J., Stragliotto, G., Tran, D. D., Brem, S., Hottinger, A. F., Kirson, E. D., Lavy-Shahaf, G., Weinberg, U., Kim, C. Y., Paek, S. H., Nicholas, G., Burna, J., Hirte, H., Weller, M., Palti, Y., Hegi, M. E., and Ram, Z. (2017). Effect of tumor-treating fields plus maintenance temozolomide vs maintenance temozolomide alone on survival in patients with glioblastoma a randomized clinical trial. *JAMA - Journal of the American Medical Association*, 318(23).

[Wongsurawat et al., 2020] Wongsurawat, T., Jenjaroenpun, P., De Loose, A., Alkam, D., Ussery, D. W., Nookaew, I., Leung, Y. K., Ho, S. M., Day, J. D., and Rodriguez, A. (2020). A novel Cas9-targeted long-read assay for simultaneous detection of IDH1/2 mutations and clinically relevant MGMT methylation in fresh biopsies of diffuse glioma. *Acta Neuropathologica Communications*, 8(1):1–13.

[Xie et al., 2015] Xie, H., Tubbs, R., and Yang, B. (2015). Detection of MGMT promoter methylation in glioblastoma using pyrosequencing. *International Journal of Clinical and Experimental Pathology*, 8(2).

[Yuan et al., 2017] Yuan, G., Niu, L., Zhang, Y., Wang, X., Ma, K., Yin, H., Dai, J., Zhou, W., and Pan, Y. (2017). Defining optimal cutoff value of MGMT promoter methylation by ROC analysis for clinical setting in glioblastoma patients. *Journal of Neuro-Oncology*, 133(1).

[Zhang et al., 2011] Zhang, J., F.G. Stevens, M., and D. Bradshaw, T. (2011). Temozolomide: Mechanisms of Action, Repair and Resistance. *Current Molecular Pharmacology*, 5(1).